Fatty Acid Imaging with ^{123}I-15-(p-Iodophenyl)-9-R,S-Methylpentadecanoic Acid in Acute Coronary Syndrome

Satomi Fujiwara, Yasuchika Takeishi, Taiki Tojo, Minako Yamaoka, Joji Nitobe, Kazuei Takahashi and Hitonobu Tomoike

First Department of Internal Medicine and Department of Radiology, Yamagata University School of Medicine, Yamagata, Japan

^{123}I-15-(p-iodophenyl)-9-R,S-methylpentadecanoic acid (9-MPA) has recently been developed as a tracer for myocardial fatty acid uptake. The aim of this study, which was performed as part of a phase III clinical trial of 9-MPA, was to test the usefulness of 9-MPA for the assessment of myocardial viability in patients with acute coronary syndrome (ACS). **Methods:** Fifteen patients with ACS who had undergone direct percutaneous transluminal coronary angioplasty were examined. Myocardial SPECT with 9-MPA and ^{99m}Tc-sestamibi and low-dose dobutamine echocardiography were performed within 2 wk after onset. The 9-MPA images were obtained 10 and 60 min after tracer administration, and sestamibi imaging was begun 60 min after the injection. The left ventricle was divided into 9 segments, and 9-MPA and sestamibi uptake were scored from 0 (normal) to 3 (no activity) in each segment. Lower uptake of 9-MPA than of sestamibi was defined as a mismatch. Myocardial segments showing improvement in wall motion during low-dose dobutamine infusion (5–10 μg/kg/min) were considered viable. **Results:** The 9-MPA images were of high quality for all patients. Myocardial uptake of 9-MPA was lower in ischemic myocardium than in nonischemic myocardium (58.2% ± 14.2% versus 91.9% ± 6.5%, $P < 0.0001$). Clearance of 9-MPA from ischemic myocardium was slower than that from nonischemic myocardium (10.2% ± 11.7% versus 19.1% ± 5.9%, $P < 0.01$). A mismatch was seen in 10 of 15 patients, and 18 of 20 (90%) mismatched segments were defined as viable by dobutamine echocardiography. Conversely, 18 of 20 (90%) matched segments did not show any improvement in function during dobutamine stimulation ($P < 0.0001$). Uptake of 9-MPA in nonviable segments was lower than that in dysfunctional but viable segments ($P < 0.05$), and 9-MPA clearance from nonviable segments was slower than that from viable segments ($P < 0.05$). **Conclusion:** The imaging characteristics of 9-MPA for SPECT are excellent, allowing noninvasive assessment of myocardial fatty acid uptake. Myocardial imaging with 9-MPA may reveal impaired fatty acid uptake in dysfunctional but viable myocardium and thus provide useful information for clinical decision making in ACS.

Key Words: ^{123}I-15-(p-iodophenyl)-9-R,S-methylpentadecanoic acid; acute coronary syndrome; fatty acid metabolism; myocardial viability; stunned myocardium

J Nucl Med 1999; 40:1999–2006

Received Nov. 24, 1998; revision accepted Apr. 9, 1999.

For correspondence or reprints contact: Satomi Fujiwara, MD, First Department of Internal Medicine, Yamagata University School of Medicine, 2-2-2 Iida-Nishi, Yamagata 990-9585, Japan.

Successful coronary reperfusion in acute coronary syndrome (ACS) accompanies functional abnormalities that will be reversible or irreversible. Although early reperfusion may increase the probability of functional amelioration, differentiation of reversible from fixed dysfunction may be difficult because functional recovery in areas salvaged by reperfusion may be delayed for several weeks (*1*). Because the prognosis correlates with ventricular function, early and accurate identification of reversible dysfunction may be of great importance for optimal management of patients with ACS. For this purpose, low-dose dobutamine echocardiography and quantitative assessment of myocardial perfusion tracer have been applied to identify viable myocardium (*2,3*).

Noninvasive assessment of myocardial metabolism with PET has also played an important role in the examination and management of patients with coronary artery disease (*4*). However, positron imaging requires a cyclotron and a positron camera and is not yet widely available because of the cost. In the clinical setting, single-photon radionuclides are also labeled to fatty acids (*5*). ^{123}I-phenylpentadecanoic acid (IPPA) and ^{123}I-beta-methyl-p-iodophenyl-pentadecanoic acid (BMIPP) have been widely used for the assessment of myocardial fatty acid uptake and metabolism (*4,5*). IPPA is a synthetic straight-chain fatty acid that is metabolized by β-oxidation (*4,5*). Thus, β-oxidation of fatty acids can be directly assessed by the clearance kinetics of IPPA. BMIPP is a modified synthetic fatty acid in which methyl branching has been introduced into the β-position to inhibit β-oxidation (*4,5*). Inhibition of β-oxidation allows prolonged myocardial retention of BMIPP, and thus tomograms of high quality can be obtained. In addition to having favorable characteristics for tomographic imaging, BMIPP has a property that benefits assessment of myocardial viability. Reduced BMIPP uptake, compared with perfusion, has been reported in patients with acute and chronic coronary artery disease (*6–12*), and this phenomenon indicates the presence of ischemic but viable myocardium. Combined BMIPP and perfusion imaging has been shown to provide more precise information on viability than does perfusion imaging alone (*6–12*).

^{123}I-15-(p-iodophenyl)-9-R,S-methylpentadecanoic acid (9-MPA) has recently been developed as another methyl-branched fatty acid tracer, with the methyl branching introduced into carbon position 9 of the fatty acid chain. Therefore, 9-MPA, as well as BMIPP, has sufficiently prolonged myocardial retention for SPECT acquisition and may have potential for detecting viable myocardium.

The aim of this study, which was performed as part of a phase III clinical trial of 9-MPA, was to test the usefulness of 9-MPA for the assessment of myocardial viability in patients with ACS. For this purpose, myocardial uptake and clearance of 9-MPA were examined in ischemic and nonischemic myocardium and compared with flow distribution assessed by ^{99m}Tc-sestamibi (sestamibi) and regional wall motion assessed by low-dose dobutamine echocardiography.

MATERIALS AND METHODS

Patients and Study Protocol

Fifteen patients with ACS were enrolled (13 men, 2 women; age range 59–80 y, mean age 63 y). Table 1 shows their characteristics. Fourteen patients had acute myocardial infarction, and 1 had unstable angina. Acute myocardial infarction was defined as either nitroglycerin-resistant chest pain persisting more than 30 min with accompanying typical ST-segment elevation or the appearance of pathologic Q waves on a 12-lead electrocardiogram and creatine kinase more than twice the normal level with more than 5% MB isoenzyme. In 1 patient who did not show a significant elevation of creatine kinase, unstable angina pectoris was diagnosed. All patients underwent direct percutaneous transluminal coronary angioplasty (PTCA) soon after admission, and coronary revascularization was successful in all. After the interventional procedures, contrast-enhanced left ventriculography was performed to assess left ventricular function. Left ventricular ejection fraction was measured by the method of Simpson (*13*) from the right anterior oblique ventriculogram. Left ventriculography was repeated during the chronic stage (mean 37 d after onset, range 14–147 d). Written informed consent was obtained from all patients, and the study protocol was approved by the institutional review board on human research.

Myocardial SPECT with 9-MPA (Daiichi Radioisotope Laboratories, Ltd., Tokyo, Japan) and sestamibi was performed within 2 wk (mean 9 d) after the onset of ACS. The 9-MPA had a specific activity of 400 MBq/mg and a radiochemical purity of more than 95%. Patients had fasted overnight and were resting when the tracers were injected. Two-dimensional echocardiography was performed on resting patients during low-dose dobutamine infusion within 7 d (mean 5 d) after the onset of ACS.

Myocardial SPECT

Imaging was performed on resting patients. A three-head rotating gamma camera (Multispect 3; Siemens Medical Systems, Chicago, IL) equipped with a low-energy, high-resolution collimator was used as previously reported (*9,10*). A dose of 166 MBq 9-MPA was injected intravenously, and SPECT images were obtained 10 and 60 min afterward. Seventy-two images were collected over a 360° arc with a 50-s acquisition time per image. Energy discrimination was provided by a 15% window centered at 159 keV. The data were stored on a 64 × 64 matrix. Data were processed on a nuclear medicine computer system (Icon; Siemens). A series of contiguous transaxial images of 6-mm thickness were reconstructed using a filtered backprojection algorithm without attenuation correction. These transaxial images were then reoriented along the short axis and vertical long axis of the left ventricle (*9,10*).

Myocardial perfusion imaging with sestamibi was performed

TABLE 1
Patient Characteristics

Patient no.	Age (y)	Sex	Diagnosis	Culprit artery	TIMI grade	Time to reperfusion (h)	Peak CK level (IU)	9-MPA uptake and clearance (%)						Mismatch	LVEF (%)		Wall motion score	
								Ischemic			Nonischemic							
								Early	Delayed	CL	Early	Delayed	CL		Acute	Chronic	Rest	DOB
1	64	M	AMI	LCx	0	5.5	1058	56	62	11	94	93	20	+	50	58	NA	NA
2	70	M	AMI	RCA	0	3.0	1989	51	58	17	92	91	29	+	NA	52	NA	NA
3	62	M	AMI	LCx	2	18.0	955	88	88	12	86	87	10	Normal	68	69	0	NA
4	79	F	AMI	LAD	2	3.0	410	78	73	25	90	93	18	+	50	58	0	NA
5	73	M	AMI	RCA	2	>24.0	823	41	50	−3	94	94	16	+	37	NA	8	6
6	78	M	AMI	RCA	0	3.5	8739	42	50	0	94	95	15	−	34	32	12	12
7	68	F	UAP	LAD	2	>24.0	231	63	63	13	91	88	16	+	52	62	1	0
8	57	M	AMI	RCA	0	>24.0	1118	45	60	−6	91	90	24	+	NA	38	4	2
9	38	M	AMI	LAD	3	>24.0	595	63	66	14	92	90	21	+	47	65	3	0
10	67	M	AMI	RCA	0	>24.0	3147	48	58	−1	94	93	18	−	51	46	4	4
11	78	M	AMI	LAD	0	4.0	2940	58	57	13	94	93	14	+	57	65	7	6
12	79	M	AMI	RCA	0	3.0	1491	71	80	17	94	98	23	+	53	64	2	0
13	71	M	AMI	LAD	0	5.5	5335	63	78	5	94	99	21	−	NA	NA	11	11
14	62	M	AMI	LAD	0	3.0	4662	55	60	20	92	96	25	−	50	54	11	11
15	58	M	AMI	LAD	3	13.0	2290	78	73	25	90	93	18	+	46	61	8	4

TIMI = Thrombolysis in Myocardial Infarction Trial; CK = creatine kinase; 9-MPA = ^{123}I-15-(p-iodophenyl)-9-R,S-methylpentadecanoic acid; CL = clearance; LVEF = left ventricular ejection fraction; DOB = dobutamine; AMI = acute myocardial infarction; LCx = left circumflex artery; + = positive; NA = not available; RCA = right coronary artery; LAD = left anterior descending artery; − = negative; UAP = unstable angina pectoris.

within 3 d before or after 9-MPA imaging. A dose of 740 MBq sestamibi was administered intravenously, and SPECT was started 60 min after the injection (*10*). The sestamibi imaging was performed in the same manner as 9-MPA imaging with the exception of a 140-keV photopeak instead of 159 keV and a 30-s acquisition time instead of 50 s.

The myocardial 9-MPA and sestamibi images were analyzed separately by two independent observers who were unaware of the patient data. The left ventricular myocardium was divided into 9 segments representing the anterior, septal, inferior and lateral walls of the basal and midventricular levels in the short-axis view and an apical segment in the vertical long-axis view (*9,10*). A four-point scoring system was applied for evaluating the segmental myocardial uptake of the tracers as previously described (*9,10*), with 0 representing normal uptake; 1, reduced uptake; 2, severely reduced uptake; and 3, no uptake. Lower uptake of 9-MPA than of sestamibi on the early image was defined as a mismatch. The grading was settled by consensus between the two observers. The vascular territories of three major coronary arteries were assigned in principle, with the anterior, septal and apical regions corresponding to the left anterior descending artery, the region inferior to the right coronary artery and the region lateral to the left circumflex artery, respectively. However, the apical region was often included in the territory of the right coronary artery because of variability in vascular supply. Ischemic myocardium was defined as regions with the lowest activity in segments perfused by the culprit coronary artery.

Myocardial slices of 9-MPA and sestamibi images were selected in the same manner as for the semiquantitative analysis, and segmental uptake of 9-MPA and sestamibi was calculated by placing two regions of interest (ROIs) on each myocardial segment. Moreover, these ROIs were identically placed on the early and delayed 9-MPA images, and clearance of 9-MPA was calculated from the segmental counts of the early and delayed images as follows: clearance (%) = (Ce − Cd × Cf) × 100/Ce and Cf = $1/(1/2)^x$, x = (Td − Te)/13.2, where Ce = early image, Cd = delayed image, Td = time for delayed image and Te = time for early image.

Low-Dose Dobutamine Echocardiography

Low-dose dobutamine echocardiography was performed using a Sonos 2500 sonography system (Hewlett-Packard Co., Andover, MA) with a 2.5-MHz transducer. The patients were examined in the left lateral decubitus position at rest and during the last 3 min of each dobutamine infusion level. After the resting images were obtained, dobutamine infusion was started at an initial dose of 5 μg/kg/min for 5 min and increased to 10 μg/kg/min for 5 min more (*3,14*). Parasternal long- and short-axis views and apical four- and two-chamber views were obtained for all patients. All echocardiographic data were videotaped for subsequent analysis. Blood pressure and electrocardiograms were monitored throughout the study. No patients were on β-blocker therapy at the time of dobutamine echocardiography.

The left ventricle in the echocardiographic images was divided into 9 segments corresponding to the scintigraphic segments (*15*). Wall motion and systolic wall thickening were evaluated semiquantitatively by two experienced observers unaware of the patients' clinical and scintigraphic data. Each segment was graded on a four-point scoring system, with 0 representing normal motion; 1, hypokinesia; 2, severe hypokinesia; and 3, akinesia or dyskinesia. Dysfunctional segments were considered viable if they showed an improvement in wall motion score of more than or equal to one grade during dobutamine infusion under resting conditions (*3,14*). Differences in interpretation were resolved by consensus between the two observers.

Statistical Analysis

Unless specified, data were reported as mean ± one SD. Continuous variables were compared by a paired or unpaired *t* test, and comparisons among three groups were performed by one-way analysis of variance followed by the Scheffé F test. Differences in proportion were examined by a χ^2 test for independence. $P < 0.05$ was considered significant.

RESULTS

The early 9-MPA images were of high quality; the delayed images had slightly more noise but were still acceptable for quantitative analysis.

Case Presentation

Myocardial tomograms of a patient (patient 12, Table 1) with acute inferior myocardial infarction are shown in Figure 1. The patient underwent direct PTCA to the right coronary artery, and coronary reflow was achieved. On the sestamibi images, the low-perfusion area was seen in the inferior wall of the left ventricle. Myocardial uptake in the inferior wall was lower on early images obtained with 9-MPA than on images obtained with sestamibi. In the images obtained at 60 min, decreased fatty acid uptake was also detectable in the inferior wall. Dobutamine echocardiography in this patient showed that severely hypokinetic wall motion in the inferior wall improved after dobutamine administration, indicating residual viability in the inferior myocardium.

Myocardial Uptake and Clearance of Tracer

Myocardial uptake and clearance of 9-MPA in the ischemic and nonischemic segments are summarized in Tables 1 and 2. Myocardial uptake of 9-MPA was lower in ischemic myocardium than in nonischemic myocardium (58.2% ± 14.2% versus 91.9% ± 6.5% on early images, $P < 0.0001$; and 63.7% ± 12.6% versus 91.7% ± 7.7% on delayed images, $P < 0.0001$). Clearance was slower from ischemic myocardium than from nonischemic myocardium (10.2% ± 11.7% versus 19.1% ± 5.9%, $P < 0.01$). These findings suggest that decreases in myocardial uptake and clearance of 9-MPA represent impaired fatty acid metabolism in ischemic myocardium.

Mismatches in Ischemic Myocardium

Of 15 patients with ACS, only 1 showed no detectable abnormality on either 9-MPA or sestamibi tomograms (Table 1). A mismatch was seen in 10 of 15 patients. The defects of the two tracers were of similar size and intensity in the remaining 4 patients.

Regional uptake of the two tracers in 135 segments was compared on a segment-by-segment basis. As shown in Table 3, myocardial distribution of both 9-MPA and sestamibi was normal in 92 segments, whereas 43 segments

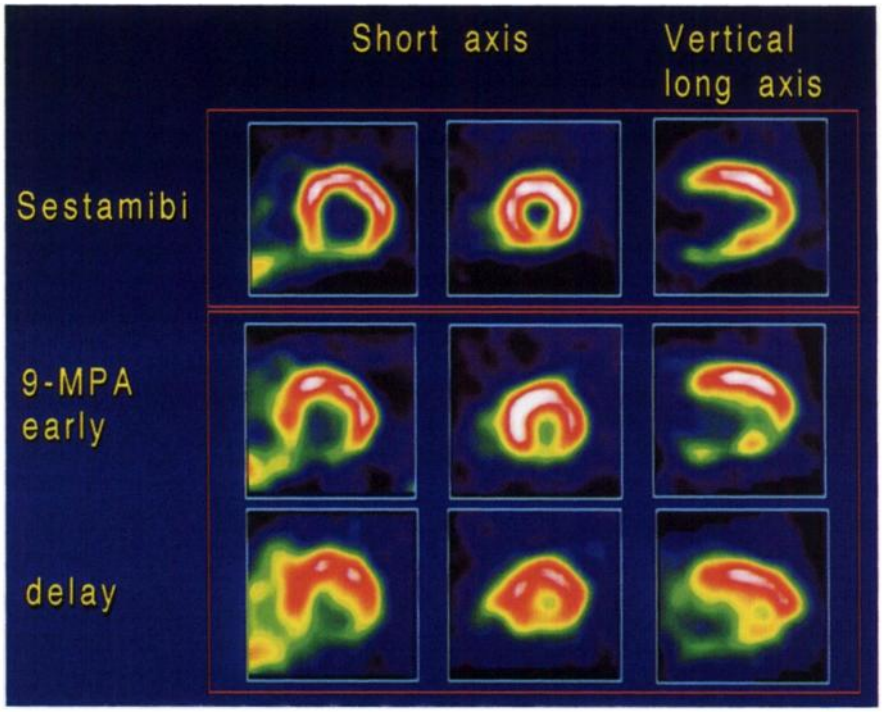

FIGURE 1. Sestamibi (top row) and 9-MPA images (middle and bottom rows) in patient with acute inferior myocardial infarction. Mismatched defect was seen in inferior myocardium.

showed heterogeneous distribution on the 9-MPA or sestamibi images. A mismatch was seen in 23 of 43 segments, whereas the defects revealed on 9-MPA and sestamibi images were of similar intensity for 20 segments. No segment showed less uptake of sestamibi than of 9-MPA.

Comparison with Dobutamine Echocardiography

Two of 15 patients had normal wall motion at rest, and 2 other patients (patients 1 and 2, Table 1) were technically poor candidates for echocardiography. Consequently, low-dose dobutamine echocardiography was performed on 11 patients; thus, 117 segments at rest and 99 segments with dobutamine infusion were analyzed for the assessment of regional wall motion. Under resting conditions, 84 segments were normokinetic, 7 were hypokinetic, 14 were severely hypokinetic and 12 were akinetic or dyskinetic. Regional wall motion improved during dobutamine infusion in 6 of 7 hypokinetic segments (86%), 6 of 14 severely hypokinetic segments (43%) and 1 of 12 akinetic or dyskinetic segments (8%) (Table 1). No myocardial segments showed deterioration in function during dobutamine infusion. Heart rate increased from 72 ± 5 beats per minute at rest to 80 ± 13 beats per minute at the peak dose infusion ($P < 0.05$). Systolic blood pressure also rose during dobutamine infusion (136 ± 18 versus 146 ± 18 mm Hg, $P < 0.05$). No patients had major side effects during the dobutamine infusion.

Of 84 myocardial segments with normal wall motion at rest, 76 (90%) showed normal 9-MPA and sestamibi uptake on tomograms (Table 4). Of the remaining 8 segments, 6 showed a mismatch. Abnormally decreased uptake of 9-MPA or sestamibi was observed in 32 of the 33 segments with abnormal wall motion. Of these 32 segments with abnormalities seen on tomograms, mismatched defects were seen in 14 and matched defects were seen in 18. Regional wall motion improved during dobutamine infusion in 12 of the 14 mismatched segments (86%), whereas none of the matched segments showed improvement with dobutamine.

As shown in Table 4, 76 of 77 segments (99%) with normal uptake of both tracers had normal wall motion at rest. Eighteen of 20 mismatched segments (90%) showed

TABLE 2
Uptake and Clearance of 9-MPA

Parameter	Ischemic	Nonischemic	*P*
Uptake (%)			
Early	58.2 ± 14.2	91.9 ± 6.5	<0.0001
Delayed	63.7 ± 12.6	91.7 ± 7.7	<0.0001
Clearance (%)	10.2 ± 11.7	19.1 ± 5.9	<0.01

9-MPA = ^{123}I-15-(p-iodophenyl)-9-R,S-methylpentadecanoic acid.

TABLE 3
Segment-by-Segment Analysis of Relative Uptake of Tracers

Early 9-MPA uptake	Sestamibi uptake			
	0	1	2	3
0	92	0	0	0
1	6	2	0	0
2	3	4	3	0
3	0	5	5	15

9-MPA = ^{123}I-15-(p-iodophenyl)-9-R,S-methylpentadecanoic acid; 0 = normal; 1 = reduced; 2 = severely reduced; 3 = none.

TABLE 4
Relation Between Relative Uptake of Tracers and Wall Motion

Wall motion	Uptake			
	Normal	Abnormal		Total
		Mismatch	Match	
Normal	76	6	2	84
Abnormal				
Viable	1	12	0	13
Nonviable	0	2	18	20
Total	77	20	20	117

either normal wall motion at rest or functional improvement during dobutamine infusion and were considered viable. Conversely, 18 of 20 matched segments (90%) had wall motion abnormalities with no functional improvement during dobutamine infusion and were considered nonviable ($P < 0.0001$ by the χ^2 test). Thus, mismatched defects had a 90% sensitivity and 90% specificity for detecting myocardial viability.

Of a total of 40 segments with mismatched and matched defects, 20 had sestamibi uptake ≥60%. Eighteen of the 20 segments were considered viable, whereas 18 of the remaining 20 segments were considered nonviable by dobutamine echocardiography. Two viable segments had sestamibi uptake <60%. Therefore, analysis of the 60% cutoff level of sestamibi uptake produced a sensitivity of 90% and a specificity of 90% for detecting viable myocardium. These findings suggest that quantitative analysis of sestamibi uptake is comparable with the combined 9-MPA and sestamibi analysis for viability assessment.

Myocardial uptake and clearance of 9-MPA were also compared with regional wall motion and functional responses to dobutamine. As shown in Figure 2, myocardial uptake seen on early 9-MPA images was more decreased in dysfunctional myocardium (viable and nonviable) than in functionally normal myocardium (90.3% ± 7.8% in normal myocardium versus 58.1% ± 9.8% in viable myocardium, $P < 0.0001$; and versus 50.6% ± 10.1% in nonviable myocardium, $P < 0.0001$). Uptake of 9-MPA was also significantly reduced in nonviable myocardium compared with that in dysfunctional but viable myocardium ($P < 0.05$). Clearance of 9-MPA was significantly slower from nonviable myocardium than from normal and viable myocardium (4.7% ± 13.4% in nonviable myocardium versus 18.1% ± 5.5% in normal myocardium, $P < 0.0001$; versus 12.3% ± 9.7% in dysfunctional but viable myocardium, $P < 0.05$). Myocardial uptake and clearance of 9-MPA were more depressed in nonviable myocardium than in viable myocardium with reversible dysfunction. These results indicate that 9-MPA imaging may identify ischemic but viable myocardium.

DISCUSSION

This study produced several major new findings. Ischemic myocardium perfused by the culprit coronary artery was found to be characterized by a decrease in myocardial uptake and clearance of 9-MPA. Mismatched defects, or lower uptake of 9-MPA than of sestamibi, were found in ischemic myocardium, and this phenomenon was associated with myocardial viability. Lower uptake and slower clearance of 9-MPA were found in nonviable myocardium than in viable myocardium.

Myocardial Fatty Acid Metabolism and Fatty Acid Tracers

Fatty acids are the principal energy source for the myocardium under normal aerobic conditions in the fasting state; however, their metabolism is suppressed and the substrate is replaced by glucose in the presence of myocardial ischemia. Therefore, assessment of myocardial metabolism has played an important role in the examination and management of patients with coronary artery disease (*4*). In the clinical setting, single-photon–emitting radionuclides are attached to fatty acids and used for fatty acid imaging (*5*). IPPA and BMIPP have been widely used in clinical and

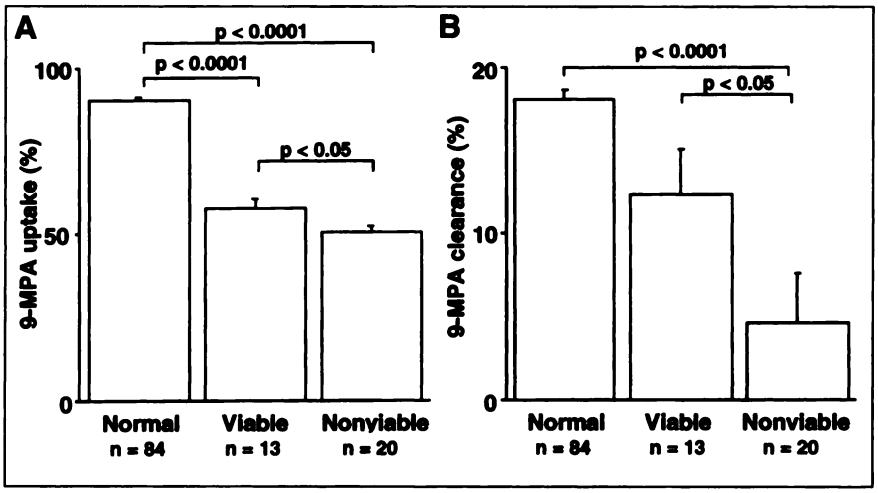

FIGURE 2. Comparisons of myocardial uptake (A) and clearance (B) of 9-MPA among functionally normal, dysfunctional but viable and nonviable myocardium. Data are reported as mean + SE.

experimental studies (*6–12,16–24*). Figure 3 shows the chemical structures of representative fatty acid tracers for PET and SPECT.

IPPA is a synthetic straight-chain fatty acid that has kinetics similar to those of the physiologic substrate, such as palmitic acid (*16*). Therefore β-oxidation of fatty acids can be directly assessed by the clearance kinetics of IPPA. However, the relatively rapid metabolism of IPPA may limit the application of IPPA to SPECT. On the other hand, excellent tomograms can be obtained with BMIPP. BMIPP is a modified synthetic fatty acid in which methyl branching has been introduced into the β-position to inhibit β-oxidation (*5,18*). Thus, BMIPP has prolonged retention in the myocardium. BMIPP is initially delivered by myocardial blood flow and trapped in the myocardium as triglycerides. A part of BMIPP is catabolized through α-oxidation followed by β-oxidation (*14,21*). BMIPP uptake has been shown to be associated with tissue adenosine triphosphate levels (*17*), triglyceride synthesis (*18*) and mitochondrial function (*22*). However, BMIPP is not metabolized directly by β-oxidation, and thus clearance from myocardium does not totally reflect β-oxidation of fatty acids.

Recently, 9-MPA has been developed as a tracer for myocardial fatty acid uptake. Methyl branching has been introduced into position 9 of the fatty acid chain. A possibility is that 9-MPA initially receives β-oxidation to the methyl-branched position because of the absence of a methyl group in the β-position. However, little is known about the myocardial kinetics of this tracer (*25*), and further investigations are needed to clarify these kinetics.

Significance of Mismatch Between Perfusion and Fatty Acid Uptake

Several clinical studies have reported a mismatch between perfusion tracer and methyl-branched fatty acid uptake. This phenomenon appeared to be less common with straight-chain fatty acids, such as IPPA and palmitate. Tateno et al. (*8*) reported that BMIPP uptake that is reduced in comparison with ^{201}Tl uptake is seen more frequently in patients with unstable angina than in patients with stable angina and that such discordant BMIPP uptake is associated with ventricular dysfunction. Franken et al. (*7*), in performing sestamibi and BMIPP imaging early after thrombolytic therapy and comparing the relative uptake of two tracers with regional wall motion, found that mismatched segments may correspond to stunned myocardium and that matched segments are associated with scar tissue. In addition, myocardium with mismatching of perfusion and BMIPP uptake has been reported to show increased ^{18}F-fluorodeoxyglucose uptake (*20*). These findings suggest that mismatching of perfusion and BMIPP uptake in patients with coronary artery disease may indicate the presence of ischemic but viable myocardium. In this study, a mismatch between perfusion and 9-MPA uptake was also shown, and this phenomenon was associated with myocardial viability. The results are consistent with the results of previous studies using BMIPP (*7,10*) but are, however, discordant with the results of studies using ^{123}I-16-iodo-3-methylhexadecanoic acid (MIHA) (*26,27*). In those studies, greater uptake of MIHA than of ^{201}Tl on redistribution or reinjection images was documented in dysfunctional but viable myocardium. Several factors may explain this discrepancy. BMIPP uptake that is reduced in comparison with perfusion has been reported to be more frequent in acute or subacute than chronic myocardial infarction and in successfully reperfused areas in which a glycolytic shift may occur for energy production. However, SPECT studies with MIHA and ^{201}Tl were performed at least 10 d after an episode of acute myocardial infarction, and most enrolled patients had significant coronary stenosis. Thus, dysfunctional myocardium would be attributed to hibernation rather than stunning in these studies. De Geeter et al. (*11*) observed BMIPP uptake that was both lower and higher than sestamibi uptake in patients with myocardial infarction. These investigators found that a mismatch was associated with coronary reperfusion in patients whose disease was in the acute stage and who had not experienced prior infarction in the territory of the culprit artery. However, BMIPP uptake that was increased in comparison with perfusion was related to occlusion of the culprit artery and previous infarction in the same territory. Recently, Hambye et al. (*12*) reported that a mismatch between perfusion and BMIPP uptake is observed in chronically ischemic but viable myocardium. Moreover, they found that a greater increase in BMIPP uptake than in perfusion is also seen in hibernating myocardium. Thus, this discrepancy could be explained not only by the different myocardial kinetics of the tracers but also by the pathophysiologic conditions of the myocardium, i.e., hibernation or stunning, the interval between the acute ischemic event and SPECT acquisition and the degree of ischemia.

A mismatch between perfusion and 9-MPA uptake was seen in functionally normal myocardium as well as in dysfunctional but viable myocardium. This finding is likely caused by recovery of wall motion in some mismatched

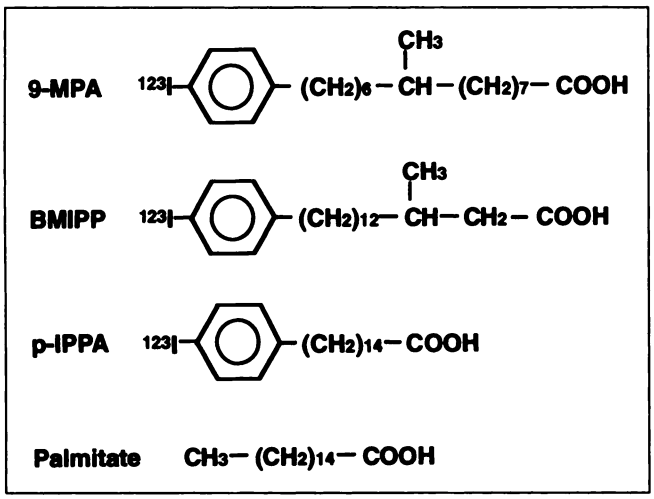

FIGURE 3. Chemical structure of 9-MPA, BMIPP, IPPA and palmitate.

segments at the time of echocardiography. In fact, all mismatched segments with normal function were perfused by the culprit artery, and left ventriculography soon after PTCA showed a wall motion abnormality in some patients with these segments. A study by Ito et al. (*28*) also supports this assumption. They reported that early restoration of coronary flow could enhance early functional recovery of postischemic myocardium.

Of 6 mismatched defects with normal wall motion and 14 with abnormal wall motion, normal sestamibi uptake was observed in 5 and 4 segments, respectively. All these segments were perfused by the culprit artery. Thus, combined 9-MPA and sestamibi imaging provides more accurate information on the area at risk than does sestamibi imaging alone.

Myocardial Uptake and Retention of 9-MPA

In this study, decreased uptake and slower clearance of 9-MPA were shown in the ischemic myocardium perfused by the culprit coronary artery. These findings are consistent with those of previous studies using IPPA and palmitic acid, which are metabolized through β-oxidation. Hansen (*23*) reported a preliminary study that showed decreased uptake and slower clearance of IPPA in dysfunctional but viable myocardium. Then, Hansen et al. (*24*) performed IPPA imaging on patients with acute myocardial infarction and found decreased uptake and clearance of IPPA in regions of infarction. These findings indicate that β-oxidation of fatty acids is suppressed in these regions. Schwaiger et al. (*29*) showed delayed metabolism of ^{11}C-palmitate in a canine model of stunned myocardium. Thus, decreased uptake and clearance of 9-MPA in this study may be associated with depressed fatty acid metabolism in the ischemic myocardium. Furthermore, myocardial uptake and clearance of 9-MPA were markedly reduced in nonviable myocardium. These results suggest that fatty acid metabolism is severely depressed or absent in nonviable myocardium.

Study Limitations

Echocardiography was not performed during the chronic stage. Therefore, whether the viable segments show functional recovery later is uncertain. However, previous studies have shown that low-dose dobutamine echocardiography predicts functional recovery well (*3,14*), and this technique is now accepted as a useful tool for assessing and predicting residual viability after acute myocardial injury. Moreover, in this study, improvement in left ventricular ejection fraction was seen in patients with a contractile response to inotropic stimulation (51% ± 4% versus 62% ± 3%, $P < 0.001$). This finding also indicates that low-dose dobutamine echocardiography is reliable for identifying reversible dysfunction. Another limitation that might have influenced the results of this study is anatomic misalignment between SPECT and echocardiographic images. However, anatomic misalignment was likely minimal because the heart was divided into 9 relatively large segments.

CONCLUSION

The imaging characteristics of 9-MPA for SPECT are excellent, allowing noninvasive assessment of myocardial fatty acid uptake. Mismatching shown by 9-MPA accurately reveals dysfunctional but viable myocardium and provides more precise information on the area at risk than does sestamibi imaging alone. Furthermore, quantitative assessment of myocardial 9-MPA uptake and clearance may distinguish dysfunctional but viable myocardium from nonviable myocardium. Myocardial imaging with 9-MPA may be useful for the detection of viable myocardium and thus has important implications for clinical decision making in ACS.

ACKNOWLEDGMENTS

This study was performed as part of a phase III clinical trial of 9-MPA. The authors thank Daiichi Radioisotope Laboratories, Ltd., for supplying the 9-MPA.

REFERENCES

1. Ellis SG, Henschke CI, Sandor T, Wynne J, Braunwald E, Kloner RA. Time course of functional and biochemical recovery of myocardium salvaged by reperfusion. *J Am Coll Cardiol.* 1983;1:1047–1055.
2. Dilsizian V, Bonow RO. Current diagnostic techniques of assessing myocardial viability in patients with hibernating and stunned myocardium. *Circulation.* 1993;87:1–20.
3. Smart SC, Sawada S, Ryan T, et al. Low-dose dobutamine echocardiography detects reversible dysfunction after thrombolytic therapy of acute myocardial infarction. *Circulation.* 1993;88:405–415.
4. Tamaki N, Fujibayashi Y, Magata Y, Yonekura Y, Konishi J. Radionuclide assessment of myocardial fatty acid metabolism by PET and SPECT. *J Nucl Cardiol.* 1995;2:256–266.
5. Knapp FF, Kropp J. Iodine-123-labelled fatty acids for myocardial single-photon emission tomography: current status and future prospectives. *Eur J Nucl Med.* 1995;22:361–381.
6. Franken PR, Dendale P, De Geeter F, Demoor D, Bossuyt A, Block P. Prediction of functional outcome after myocardial infarction using BMIPP and sestamibi scintigraphy. *J Nucl Med.* 1996;37:718–722.
7. Franken PR, De Geeter F, Dendale P, Demoor D, Block P, Bossuyt A. Abnormal free fatty acid uptake in subacute myocardial infarction after coronary thrombolysis: correlation with wall motion and inotropic reserve. *J Nucl Med.* 1994;35:1758–1765.
8. Tateno M, Tamaki N, Yukihiro M, et al. Assessment of fatty acid uptake in ischemic heart disease without myocardial infarction. *J Nucl Med.* 1996;37:1981–1985.
9. Takeishi Y, Fujiwara S, Atsumi H, Takahashi K, Sukekawa H, Tomoike H. Iodine-123-BMIPP imaging in unstable angina: a guide for interventional strategy. *J Nucl Med.* 1997;38:1407–1411.
10. Fujiwara S, Takeishi Y, Atsumi H, et al. Prediction of functional recovery in acute myocardial infarction: comparison between sestamibi reverse redistribution and sestamibi/BMIPP mismatch. *J Nucl Cardiol.* 1998;5:119–127.
11. De Geeter F, Franken PR, Knapp FF Jr, Bossuyt A. Relationship between blood flow and fatty acid metabolism in subacute myocardial infarction: a study by means of Tc-99m sestamibi and I-123-beta-methyl-iodo-phenyl pentadecanoic acid. *Eur J Nucl Med.* 1994;21:283–291.
12. Hambye ASE, Vaerenberg MM, Dobbeleir AA, Van den Heuvel PA, Franken PR. Abnormal BMIPP uptake in chronically dysfunctional myocardial segments: correlation with contractile response to low-dose dobutamine. *J Nucl Med.* 1998;39:1845–1850.
13. Chapman CB, Baker O, Reynolds J, Bonte FJ. Use of biplane cinefluorography for measurement of ventricular volume. *Circulation.* 1958;18:1105–1117.
14. Pierard LA, De Landsheere CM, Berthe C, Rigo P, Kulbertus HE. Identification of viable myocardium by echocardiography during dobutamine infusion in patients with myocardial infarction after thrombolytic therapy: comparison with positron emission tomography. *J Am Coll Cardiol.* 1990;15:1021–1031.
15. Takeishi Y, Chiba J, Abe S, Ikeda K, Tomoike H. Adenosine-echocardiography for the detection of coronary artery disease. *J Cardiol.* 1994;24:1–7.

16. Reske SN, Sauer W, Machulla HJ, Winkler C. 15(p-^{123}I-iodophenyl)pentadecanoic acid as tracer of lipid metabolism: comparison with [1-^{14}C]palmitic acid in murine tissues. *J Nucl Med.* 1984;25:1335–1342.
17. Fujibayashi Y, Yonekura Y, Takemura Y, et al. Myocardial accumulation of iodinated beta-methyl-branched fatty acid analogue, iodine-125–15-(p-iodophenyl)-3-(R,S)methylpentadecanoic acid (BMIPP), in relation to ATP concentration. *J Nucl Med.* 1990;31:1818–1822.
18. Knapp FF, Kropp J, Goodman M, et al. The development of iodine-123-methyl-branched fatty acids and their applications in nuclear cardiology. *Ann Nucl Med.* 1993;7(suppl):S1–S14.
19. Yamamichi Y, Kusuoka H, Morishita K, et al. Metabolism of iodine-123-BMIPP in perfused rat hearts. *J Nucl Med.* 1995;36:1043–1050.
20. Tamaki N, Tadamura E, Kawamoto M, et al. Decreased uptake of iodinated branched fatty acid analog indicates metabolic alterations in ischemic myocardium. *J Nucl Med.* 1995;36:1974–1980.
21. Fujibayashi Y, Nohara R, Hosokawa R, et al. Metabolism and kinetics of iodine-123-BMIPP in canine myocardium. *J Nucl Med.* 1996;37:757–761.
22. Hosokawa R, Nohara R, Fujibayashi Y, et al. Metabolic fate of iodine-123-BMIPP in canine myocardium after administration of etomoxir. *J Nucl Med.* 1996;37:1836–1840.
23. Hansen CL. Preliminary report of an ongoing phase I/II dose range, safety and efficacy study of iodine-123-phenylpentadecanoic acid for the identification of viable myocardium. *J Nucl Med.* 1994;35(suppl):38S–42S.
24. Hansen CL, Kulkarni PV, Ugolini V, Corbett JR. Detection of alterations in left ventricular fatty acid metabolism in patients with acute myocardial infarction by 15-(p-I-123-phenyl)-pentadecanoic acid and tomographic imaging. *Am Heart J.* 1995;129:476–481.
25. Chouraqui P, Maddahi J, Henkin R, Karesh SM, Galie E, Berman DS. Comparison of myocardial imaging with iodine-123-iodophenyl-9-methyl pentadecanoic acid and thallium-201-chloride for assessment of patients with exercise-induced myocardial ischemia. *J Nucl Med.* 1991;32:447–452.
26. Marie PY, Karcher G, Danchin N, et al. Thallium-201 rest-reinjection and iodine-123-MIHA imaging of myocardial infarction: analysis of defect reversibility. *J Nucl Med.* 1995;36:1561–1568.
27. Marie PY, Angioi M, Danchin N, et al. Assessment of myocardial viability in patients with previous myocardial infarction by using single-photon emission computed tomography with a new metabolic tracer: [I-123]-16-iodo-3-methylhexadecanoic acid (MIHA)—comparison with the rest-reinjection thallium-201 technique. *J Am Coll Cardiol.* 1997;30:1241–1248.
28. Ito H, Tomooka T, Sakai N, et al. Time course of functional improvement in stunned myocardium in risk area in patients with reperfused anterior infarction. *Circulation.* 1993;87:355–362.
29. Schwaiger M, Schelbert HR, Keen R, et al. Retention and clearance of C-11 palmitic acid in ischemic and reperfused canine myocardium. *J Am Coll Cardiol.* 1985;6:311–320.